JACS
JOURNAL OF THE AMERICAN CHEMICAL SOCIETY
Article
pubs.acs.org/JACS

Experimental and Computational Studies on the [3,3]- and [3,5]-Sigmatropic Rearrangements of Acetoxycyclohexadienones: A Non-ionic Mechanism for Acyl Migration

Shikha Sharma,[†] Trideep Rajale,[†] David B. Cordes,[‡] Fernando Hung-Low, and David M. Birney*

Department of Chemistry and Biochemistry, Texas Tech University, Lubbock, Texas 79409-1061, United States

Supporting Information

ABSTRACT: Flash vacuum pyrolysis studies of substituted 6-acetoxy-2,4-cyclohexadienones (**3** and **10**) from 300 to 500 °C provide strong experimental evidence that direct [3,5]-sigmatropic rearrangements in these molecules are favored over the more familiar [3,3]-sigmatropic rearrangements. The preference holds when the results are extrapolated to 0.0% conversion, indicating that this is a concerted process. Pyrolysis of 6,6-diacetoxy-2-methyl-2,4-cyclohexadienone (**9**) at 350 °C gives a modest yield of the initial [3,5]-sigmatropic rearrangement product, 2,6-diacetoxy-6-methyl-2,4-cyclohexadienone (**11**). Qualitative arguments and electronic structure theory calculations are in agreement that the lowest energy pathway for each [3,5]-sigmatropic rearrangement is via an allowed, concerted pseudopericyclic transition state. The crystal structures of compounds **3**, **9**, and **10** prefigure these transition states. The selectivity for the [3,5] products increases with an increasing temperature. This unexpected selectivity is explained by a concerted, intramolecular, and pseudopericyclic transition state (**TS-5**) that forms a tetrahedral interemediate (*ortho*-acid ester **4′**), followed by similar ring openings to isomeric phenols, which shifts the equilibrium toward the phenols from the [3,5] (but not the [3,3]) products.

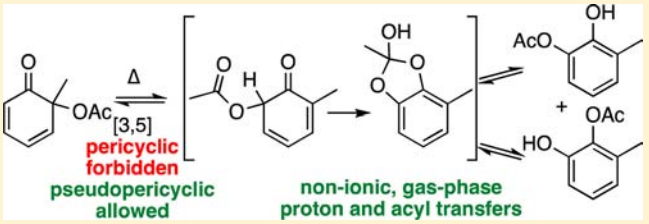

INTRODUCTION

One of the salient characteristics of concerted pericyclic reactions is the alternation of allowed and forbidden pathways, depending upon the number of electrons in the loop of interacting orbitals.[1] Thus, [3s,3s]-sigmatropic rearrangements (e.g., the Cope rearrangement) are allowed, while [3s,5s]-sigmatropic rearrangements are forbidden thermally and are calculated to have higher reaction barriers and proceed via biradical intermediates (Scheme 1).[2]

Scheme 1. Calculated (B3LYP/6-31G*) Energies for the Forbidden and, Therefore, Stepwise [3s,5s]-Sigmatropic Rearrangement and the Allowed and, Therefore, Concerted [3s,3s]-Sigmatropic Rearrangement of 1,3,7-Octatriene[2]

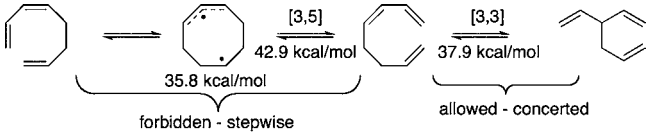

In contrast, pseudopericyclic reactions are orbital-symmetry-allowed, regardless of the number of atoms involved.[3] This is because pseudopericyclic reactions, although having concerted bond changes around a ring, lack the cyclic orbital overlap that is characteristic of a pericyclic reaction. Pseudo-pericyclic reactions also tend to have planar transition states and lower barriers than model pericyclic reactions.[4] We have recently performed a multiphoton infrared (MP-IR) study that demonstrated that eight-centered δ-elimination in *Z*-2-acetoxy-3-pentene (*cis*-**1**) to directly form *trans*-**2** is competitive with the more familiar six-centered β-elimination to form *cis*-**2** (Scheme 2).[4i] In separate work, we have shown computationally [*ab initio* and density functional theory (DFT) calculations] that sigmatropic rearrangements of esters are pseudopericyclic and, hence, the [3,3]- and [3,5]-sigmatropic rearrangements are competitive.[4c,d] In both of these systems, the bond formation and breaking is calculated to occur in the plane of the ester and the ester π system does not participate.

Scheme 2. Initial Product Distribution from MP-IR Irradiation of *Z*-2-Acetoxy-3-pentene (*cis*-1)[4i]

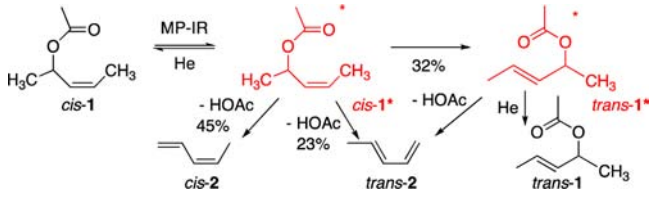

In the current work, we undertook a detailed experimental and computational study to explore the [3,3]- and [3,5]-

Received: July 26, 2013
Published: August 22, 2013

   dx.doi.org/10.1021/ja4077364 | J. Am. Chem. Soc. 2013, 135, 14438−14447

sigmatropic rearrangements of a few representative *o*-quinol acetate (6-acetoxy-2,4-cyclohexadieneone) derivatives (e.g., compound **3** in Scheme 3). These are obtained after the

Scheme 3

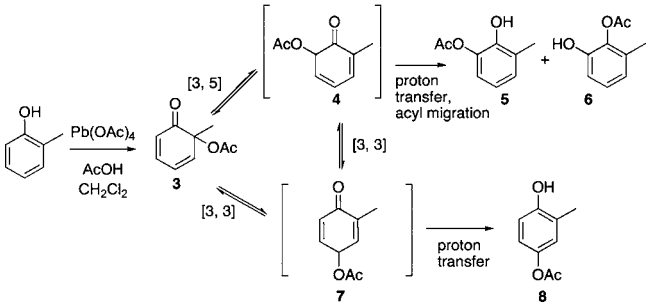

oxidative dearomatization of phenols, and they as well as their [3,3]- and [3,5]-rearranged products are of great synthetic utility, because they have been used to prepare polyoxygenated compounds as well as intermediates in the synthesis of a number of natural products.[4d,5,6] These experimental results led us to use computational methods to explore a gas-phase, unimolecular proton transfer mechanism for aromatization of the initial products of rearrangement (e.g., compounds **5** and **7**). Somewhat to our surprise, we found a non-ionic, concerted, pseudopericyclic transition state for this process, as well as a similar one for acyl migration in the *o*-acetoxyphenols (e.g., compounds **5** and **6**).

[3,5]-Sigmatropic Rearrangements of Esters: Allowed or Forbidden? Oxidation of phenols using lead(IV) acetate (in acetic acid) or iodobenzene diacetate gives acetoxycyclohexadienones.[5,6] Wessely and co-workers used lead(IV) acetate to synthesize a number of cyclohexadienone derivatives and studied their facile thermal rearrangements.[6] Phenols **5** and **6** were the major products obtained after pyrolysis of compound **3**, in 4-fold excess over compound **8** (Scheme 3). In 1961, Wessely and co-workers suggested that compounds **5** and **6** could arise from a [3,5]-sigmatropic rearrangement of compound **3** to give compound **4** followed by tautomerization to the phenols and transesterification, although he recognized that two sequential [3,3]-sigmatropic rearrangements via compounds **7** and **4** would give the same products.[6d] The subsequent publication of the Woodward–Hoffmann rules led others to favor the latter mechanism with two sequential [3,3]-sigmatropic rearrangements.[1b] A [3,5]-sigmatropic rearrangement as proposed by Wessely and co-workers[6d] would be geometrically constrained to be suprafacial on both components and, therefore, would not be allowed according to the orbital symmetry rules.

However, calculations from the Birney and Quideau groups[4c,d] have supported the initial proposal by Wessely and co-workers for a concerted transition state for this type of [3,5]-sigmatropic rearrangement. 2,4-Cyclohexadienyl formate was first examined as a model system. At the B3LYP/6-31G(d,p) level, a pseudopericyclic transition state was located for the [3,5]-sigmatropic rearrangement. At this level of theory, it was 3.0 kcal/mol lower in energy than the competing [3,3]-sigmatropic rearrangement (Scheme 4a). The [3,5]-sigmatropic rearrangement transition state is calculated to be planar on the ester (bond forming and breaking occurs in the O–C=O plane). The [3,3] transition state geometry is similar to the boat geometry of a Cope rearrangement but is somewhat flattened at

Scheme 4

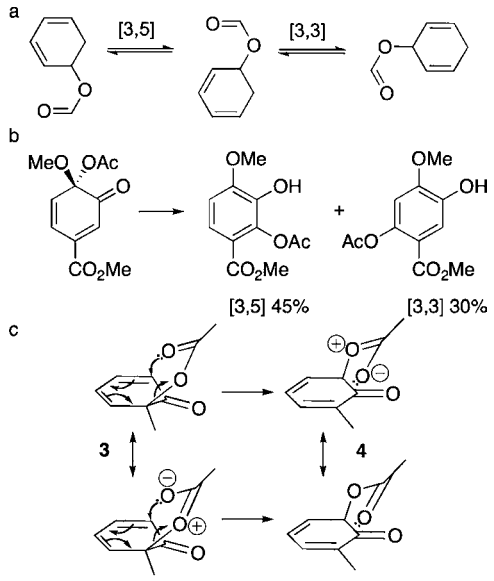

the ester.[4c] Additional calculations on the experimental system in Scheme 4b were in accordance with the experimental preference for [3,5]-sigmatropic rearrangement.[4d] Scheme 4c shows a simple resonance way of visualizing the orbital disconnections in the reaction from compound **3** to compound **4**; it is possible to move the electrons from the breaking and forming σ bonds separately from the π-electron system of the ester functional group. This illustrates that there are disconnections on the ester oxygens; this means that the [3,5]-sigmatropic rearrangement is pseudopericyclic and, therefore, allowed.

Nevertheless, an experimental distinction between the two mechanisms (either sequential [3,3]-sigmatropic rearrangements via compound **7** to compound **4** or direct [3,5]-sigmatropic rearrangement to compound **4**) has remained lacking. Therefore, we undertook a combined experimental and computational study of the thermal rearrangement of compound **3** as well as the related compounds **9** and **10**. Compounds **3**, **9**, and **10** were synthesized following modified literature precedents, by lead(IV) acetate oxidation of the appropriately substituted phenols (Scheme 5).[6] Full experimental details are provided in the Supporting Information.

Scheme 5

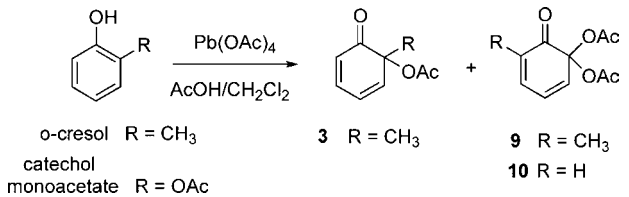

RESULTS AND DISCUSSION

Flash vacuum pyrolysis (FVP, also known as flash vacuum thermolysis) has proven to be a powerful technique to study organic reaction mechanisms, generate reactive intermediates, and synthesize new compounds on a preparative scale.[7] It is particularly useful for the study of unimolecular gas-phase reactions. In the absence of solvents, ionic mechanisms can be

dx.doi.org/10.1021/ja4077364 | J. Am. Chem. Soc. 2013, 135, 14438–14447

ruled out. This method can be considered to be a greener alternative to the reactions carried out in high-boiling-point solvents.[7c]

Acetoxycyclohexadienones **3**, **9**, and **10** were subjected to FVP at a series of temperatures (Scheme 6). The products were

Scheme 6

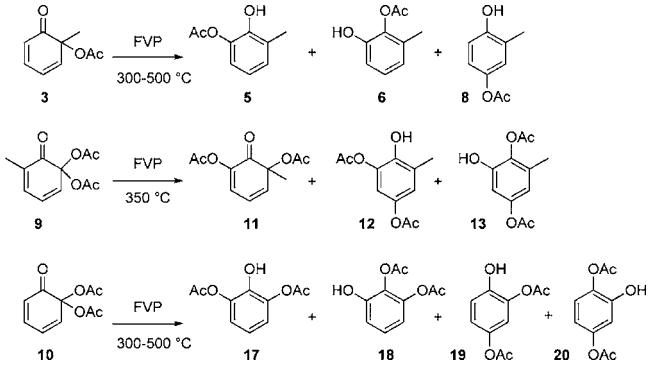

first collected in a cold trap, separated by column chromatography, and then identified by nuclear magnetic resonance (NMR). The pairs of *o*-acetoxyphenols (e.g., compounds **5** and **6**, compounds **12** and **13**, compounds **17** and **18**, or compounds **19** and **20**) interconverted upon standing (this will be discussed in more detail below). Because each pair corresponds to the same rearrangement ([3,5] or [3,3]), the sum of the individual compounds will be discussed below. The product mixture from compound **3** was difficult to quantify by gas chromatography (GC) analysis because of overlapping peaks and because of the interconversion. Therefore, the crude reaction products from FVP of compound **3** were trimethylsilylated prior to quantitative GC analysis (see the Supporting Information).[8] In the subsequent discussions, the GC integrations will be referred to as the parent phenols, even though the analysis was performed after silylation. The FVP was performed in triplicate at each temperature, and all results are shown (overlapping) in the figures.

FVP of Compound 3. The results from the FVP studies on compound **3** are summarized in Figure 1. The percentages of unreacted compound **3**, the [3,3]-sigmatropic rearrangement product **8**, and the sum of the [3,5]-sigmatropic rearrangement

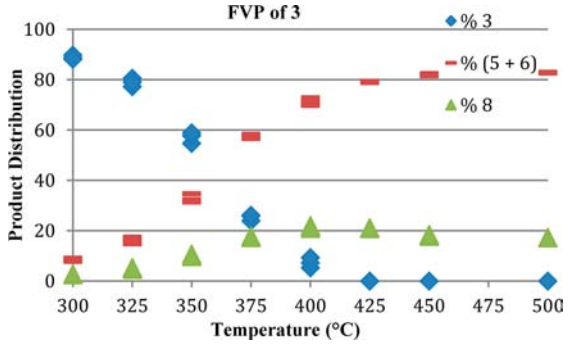

Figure 1. Product distribution from FVP of compound **3** versus temperature. Percent reactant (compound **3**) and products from GC analysis (see the text for details). Results from three repetitions are shown (overlapping). The yield of the [3,5]-sigmatropic rearrangement is the sum of the yields of compounds **5** and **6**, and the yield of the [3,3]-sigmatropic rearrangement product **8** is shown separately.

products **5** and **6** are plotted versus FVP temperature. Significantly, at all temperatures, more [3,5]-sigmatropic rearrangement products are observed than [3,3]-sigmatropic rearrangement product, in accordance with the qualitative theory that all pseudopericyclic reactions are allowed. The ratio of compounds **5**/**6** ranged from 5:1 to 8:1, but there was no clear trend as a function of the temperature (see Figure S1 of the Supporting Information).

The first question was to determine the initial ratio of [3,5]-sigmatropic rearrangement to [3,3]-sigmatropic rearrangement. When this ratio is plotted versus percent conversion for FVP between 300 and 400 °C (Figure 2) and extrapolated to 0.0%

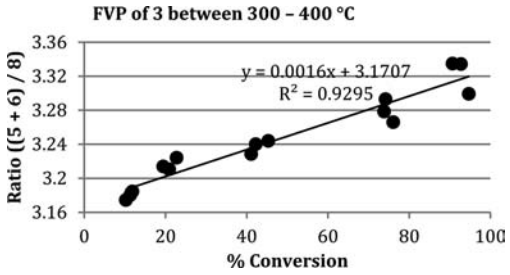

Figure 2. Ratio of [3,5]-sigmatropic rearrangement products (sum of compounds **5** and **6**) and [3,3]-sigmatropic rearrangement product (compound **8**) from FVP of compound **3** over the temperature range of 300–400 °C as a function of percent conversion. The line is a linear fit to this selected portion of the data.

conversion, it predicts an initial product distribution of 3.17:1 favoring the [3,5]-sigmatropic rearrangement from compound **3** to compound **4**. This ratio is comparable to the "adjusted" 4:1 ratio reported by Wessely and co-workers after vacuum pyrolysis of compound **3** at 450 °C.[6] The major products are allowed via a pseudopericyclic process but forbidden as a [3s,5s]-pericyclic process, and the formally allowed [3s,5a]- or [3a,5s]-antarafacial processes are not geometrically accessible. Because the majority of the initial products are from a [3,5] process, this argues for the pseudopericyclic pathway.

However, the temperature dependence of the [3,5]/[3,3] ratio in Figure 2 was unexpected and puzzled us for some time. As the temperature is increased, the selectivity for [3,5]-sigmatropic rearrangement products increases. Three mechanistic possibilities are considered here and outlined in Scheme 7: competing unimolecular reactions (Scheme 7a), an approach to equilibrium (Scheme 7b), and equilibration followed by an irreversible reaction of compound **4** (Scheme 7c).

Scheme 7. Possible Mechanistic Pathways for the Formation of Compounds 4 and 7 in the Thermal Rearrangement of Compound 3: (a) Competing Unimolecular Reactions, (b) Approach to Equilibrium, and (c) Equilibration with Subsequent Irreversible Reaction of Compound 4 to Compound 4′

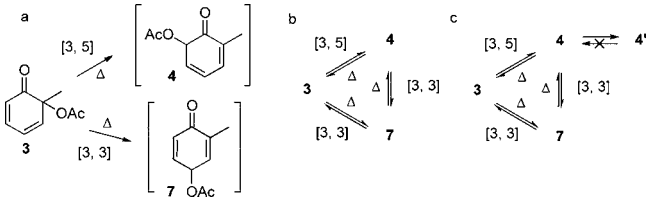

dx.doi.org/10.1021/ja4077364 | J. Am. Chem. Soc. 2013, 135, 14438–14447

Our initial expectation was that there would be a simple competition between two unimolecular reactions to give compounds **4** and **7** (Scheme 7a). Assuming that the phenol products (compounds **5**, **6**, and **8**) arise by an ionic mechanism after the FVP products are condensed, then the observed product ratios would reflect the kinetic distribution of compounds **4** and **7** under FVP conditions. Indeed, the extrapolated ratio (0.0% conversion) of 3.17:1 for [3,5]- versus [3,3]-sigmatropic rearrangement products (Figure 2) requires that the barrier for the formation of compound **4** be lower than that for compound **7**. However, if the mechanism only consists of competing unimolecular reactions, then the selectivity must decrease as the temperature is increased. This is not consistent with the increased proportion of compounds **5** and **6** ([3,5]-sigmatropic rearrangement products) relative to compound **8** seen in Figures 2 and 3.

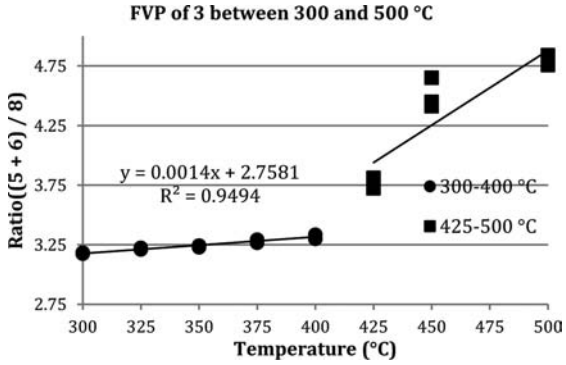

Figure 3. Product ratio of [3,5]-sigmatropic rearrangement products (sum of compounds **5** and **6**) and [3,3]-sigmatropic rearrangement product (compound **8**) from FVP of compound **3** over the temperature ranges of 300−400 and 425−500 °C as a function of temperature.

Alternatively, an approach to equilibrium between compounds **3**, **4**, and **7**, which favors compound **4**, could be proposed (Scheme 7b). Because there is no starting material **3** remaining above 400 °C, this would require that compound **4** would be significantly stabilized relative to compound **3**. It is difficult to suggest structural factors in compound **4** that would account for this. Setting aside this difficulty for the moment, this mechanistic hypothesis would be consistent with the results in Figure 2, for the limited temperature range of 300−400 °C, in that higher temperatures would bring the system closer to equilibrium and, thus, might favor the formation of compound **4** and ultimately compounds **5** and **6**.

When all of the reactant **3** has been consumed (at 425 °C and above; see Figure 1) and the equilibrium in Scheme 7b has been established, the selectivity should again decrease as the temperature is increased. However, the proportion of [3,5] products **5** and **6** increases even more dramatically as the temperature increases. This is what is observed in Figure 3, which plots the ratio of [3, 5]/[3,3] products [(**5** + **6**)/**8**] as a function of temperature. The data in the temperature range of 300−400 °C is well fit by a straight line, but the data above 400 °C is not on the same line. Therefore, these results indicate that something more than an approach to equilibrium is required for the mechanism.

The third mechanistic possibility that we considered is that there might be an approach to equilibrium between compounds **3**, **4**, and **7** but that there was also an irreversible reaction that removed compound **4** from the equilibrating system (Scheme 7c). Although we initially had no idea what the gas-phase reaction of compound **4** to compound **4′** might be, this general mechanism fits with the observed product distribution as a function of temperature. Specifically, the barrier for the formation of compound **4** would have to be lower than that for the formation of compound **7**. Both reactions could be reversible; therefore, from 300 to 400 °C, there could be some equilibration between newly formed compound **7** and starting material **3**. However, as compound **4** is formed, it could react to form compound **4′** as well as return to compound **3**. Thus, as the temperature is raised, equilibration would begin to increase compound **4** at the expense of compound **7**. Above 400 °C, all of the starting material **3** has been consumed, and as compounds **4** and **7** continue to equilibrate, the formation of **4′** would shift the equilibrium away from compound **7**. Indeed, Figure 1 shows that the proportion of compound **8** decreases at temperatures above 400 °C. This mechanism offers the only explanation of the increased ratio of [3,5]/[3,3] products [(**5** + **6**) versus **8**] at 425−500 °C. DFT calculations described below were able to identify the pathways that lead to compound **4′** and subsequently form and interconvert compounds **5** and **6**.

FVP of Compound 9. Compound **9** was obtained as a minor byproduct in the lead(IV) acetate oxidation of *o*-cresol. FVP of compound **9** at 350 °C (Scheme 8) resulted in the

Scheme 8

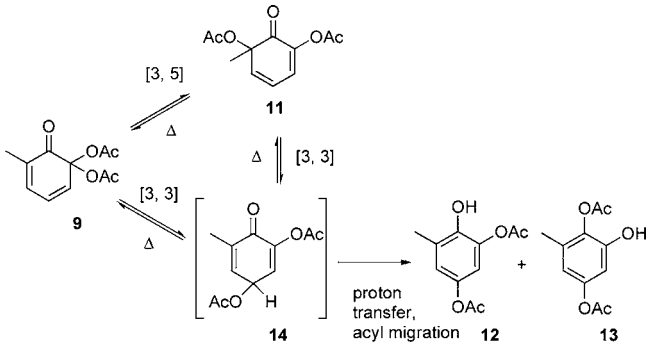

formation of both the [3,5]-sigmatropic rearrangement product **11** as well as the [3,3]-sigmatropic rearrangement product **13** (there was some evidence for the isomer **12** in the crude NMR, but only compound **13** was isolated after purification by diethyl ether washings). The intermediacy of rearranged cyclohexadieneones (e.g., compounds **4**, **7**, **11**, **14**, **15**, and **16**) seems required in any mechanism, but the observation of the [3,5] product **11** is nevertheless a reassuring confirmation.

FVP of Compound 10. The FVP of compound **10** was also carried out at temperatures ranging from 300 to 500 °C, and the product distribution (Scheme 9) was analyzed in the same manner as compound **3**. Similar to the FVP of compound **3**, the [3,5]-sigmatropic rearrangement products **17** and **18** are favored relative to the [3,3]-sigmatropic rearrangement products **19** and **20**. However, the ratio of [3,5]/[3,3] products was only about 1.2:1 at temperatures ranging from 300 to 400 °C. Again, as the temperature is raised from 425 to 500 °C, there is a significant increase in the ratio of [3,5]/[3,3] products (from 1.26 to 2.6; see Figures 4−6). These results are consistent with the mechanism proposed in Scheme 7c, an approach to equilibrium between compounds **10**, **15**, and **16**, in

dx.doi.org/10.1021/ja4077364 | J. Am. Chem. Soc. 2013, 135, 14438−14447

Scheme 9

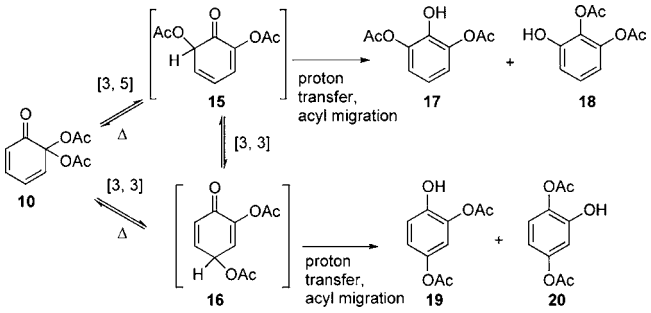

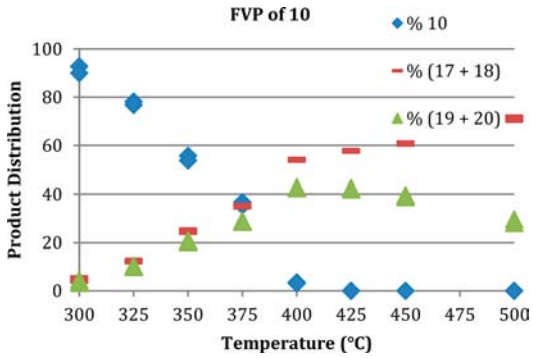

Figure 4. Product distribution from FVP of compound **10** versus temperature. Distribution of reactant (compound **10**) and products (sum of compounds **17** and **18** and compounds **19** and **20**). See Figure 1 and the text for details.

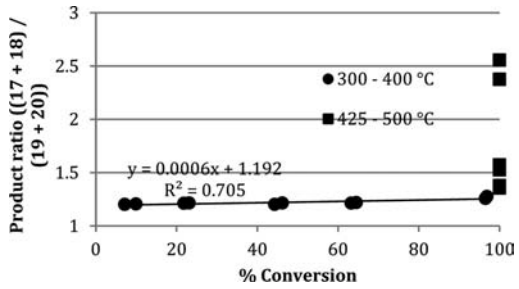

Figure 5. Ratio of [3,5]-sigmatropic rearrangement products (sum of compounds **17** and **18**) and [3,3]-sigmatropic rearrangement product (sum of compounds **19** and **20**) from FVP of compound **10** over temperature ranges of 300−400 and 425−500 °C as a function of percent conversion.

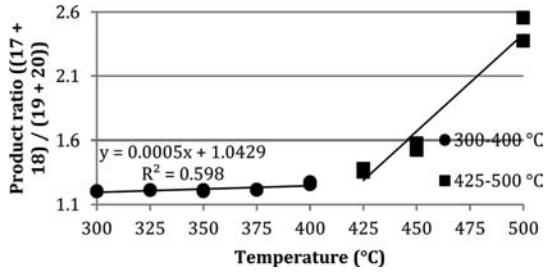

Figure 6. Product ratio of [3,5]-sigmatropic rearrangement products (sum of compounds **17** and **18**) and [3,3]-sigmatropic rearrangement product (sum of compounds **19** and **20**) over the temperature range of 300−500 °C as a function of temperature.

conjunction with an irreversible reaction of compound **15** on the way to formation of compounds **17** and **18**.

COMPUTATIONAL RESULTS

We have previously argued, on the basis of qualitative theory, electronic structure calculations, and experimental results, that [3,5]-sigmatropic rearrangements of esters are allowed via a pseudopericyclic pathway involving the in-plane σ bond and a lone pair on the ester carbonyl but not the ester π system.[4c,d] The studies reported here on the FVP of compounds **3** and **10** show that the [3,5]-sigmatropic rearrangements are favored over the competing [3,3]-sigmatropic rearrangements. The results also require irreversible gas-phase reactions of compounds **4** and **15** that shift the equilibrium toward the [3,5] products. We undertook a computational study of these three ester systems **3**, **9**, and **10**, to see if the qualitative experimental preference for [3,5]-sigmatropic rearrangements could be reproduced and also to search for a mechanism that would explain the increase in selectivity as the FVP temperatures were increased. In doing so, we found an unprecedented unimolecular, gas-phase (non-ionic) pathway that led to the formation of both isomers of the *o*-acetoxyphenol products, as will be described below.

The DFT calculations were carried out using the Gaussian03 suite of programs.[9] The geometries of the reactants, intermediates, transition states, and products were optimized using the B3LYP functional using the 6-31G(d,p) as the basis set. Transition states and minima were verified by frequency calculations. Single-point energy calculations were carried out at the B3LYP optimized geometries using the CCSD(T)/6-31G(d,p) level of theory with the NWChem electronic structure computer program.[10] Multiple conformations were calculated, when appropriate; the relative energies of the lowest energy conformations are reported in Table 1 for structures related to compound **3** and presented graphically in Figures 7, 10, and 11, for reactions of compounds **3**, **9**, and **10**, respectively. Transition states are indicated as **TS**, numbered independently and identified with the description of the rearrangement, if appropriate. Unless otherwise stated, the energies discussed below are CCSD(T) single-point energies, with B3LYP zero-point vibrational energy corrections. Intrinsic reaction coordinate (IRC) calculations were performed to confirm that the transition states (**TS5** and **TS7**) are connected with their corresponding reactants and products. Further computational details and geometries of all structures are provided in the Supporting Information.

Reactions of Compound 3. The most extensive calculations were performed for the reactions of compound **3** and are discussed below. The relative energies are summarized in Table 1 and Figure 7. Geometries of transition states related to compound **3** are shown in Figures 8 and 9.

Figure 7 summarizes the calculated energies of the reactants and products and the calculated barriers for each transition state. The [3,3]-sigmatropic rearrangement product **7** is formed via [3,3]-**TS1** with a calculated barrier of 40.6 kcal/mol. The barrier calculated for the concerted pathway for the formation of compound **4** is lower, 39.0 kcal/mol. This is consistent with the experimental observation that direct [3,5]-sigmatropic rearrangement is favored.

As was pointed out earlier (Scheme 3), the [3,5] product **4** can be formed either in a concerted manner via eight-centered [3,5]-**TS2** or by two sequential transition states, i.e., [3,3]-**TS1** followed by [3,3]-**TS3**. However, the overall barrier for the two sequential [3,3]-sigmatropic rearrangements is 43.4 kcal/mol ([3,3]-**TS3**), which is higher than either [3,5]-**TS2** or [3,3]-**TS1**. This is consistent with the experimentally observed 3.17:1 preference for [3,5]-sigmatropic rearrangement. This also suggests that equilibration (Scheme 7c) occurs primarily through compound **3** rather than directly between compounds **7** and **4**.

Figure 8 shows top and side views of the B3LYP/6-31G(d,p) optimized geometries of [3,3]-**TS1**, [3,5]-**TS2**, and [3,3]-**TS3**. The transition states for the [3,3]-sigmatropic rearrangements ([3,3]-**TS1** and [3,3]-**TS3**) are similar to the flattened boat transition states found in other ester rearrangements.[4i] We have suggested that this geometry reflects a mixing of the two orbital-symmetry-allowed possibilities: the boat [3s,3s] and pseudopericyclic geometries. As expected, [3,5]-**TS2** has no pericyclic contribution and is planar, with bond-breaking and

dx.doi.org/10.1021/ja4077364 | J. Am. Chem. Soc. 2013, 135, 14438−14447

Table 1. Relative Energies (in kcal/mol) of the Most Stable Conformers of the Starting Material and Products and Transition States for [3,3]- and [3,5]-Sigmatropic Rearrangements of Compound 3 and Subsequent Reactions

	low frequency[a,b]	DFT[b]	CCSD(T)[c]	B3LYP ZPVE[d]	CCST(T) ZPVE[d]
3	53.9	0.0	0.0	0.00	0.00
7	32.6	−3.8	−0.6	−3.8	−0.6
4	46.4	−2.7	1.0	−2.7	1.0
[3,3]-**TS1**	289.6i	36.2	42.6	34.3	40.6
[3,5]-**TS2**	287.5i	31.8	40.8	30.0	39.0
[3,3]-**TS3**	331.7i	38.0	45.2	36.2	43.4
TS4	138.1i	35.8	46.3	34.4	44.9
7′	52.7	35.2	48.5	34.4	47.8
TS5	1043.2i	23.9	31.6	21.4	29.1
4′	30.9	−15.7	−9.4	−14.6	−8.4
TS6	207.3i	−12.9	−7.0	−12.2	−6.3
TS7	395.6i	15.3	26.1	14.3	25.1
TS8	405.4i	15.6	26.6	14.6	25.6
8	23.6	−20.9	−12.9	−20.7	−12.7
5	51.2	−23.9	−15.8	−23.3	−15.1
6	43	−23.4	−15.4	−22.7	−14.8

[a]Low or imaginary frequencies (cm^{-1}) of calculated minima and transition states. [b]Optimized at the B3LYP/6-31G(d,p) level of theory. [c]CCSD(T)/6-31G(d,p) single-point energy calculations. [d]Zero-point vibrational energy (ZPVE) corrections are at the B3LYP/6-31G(d,p) level of theory.

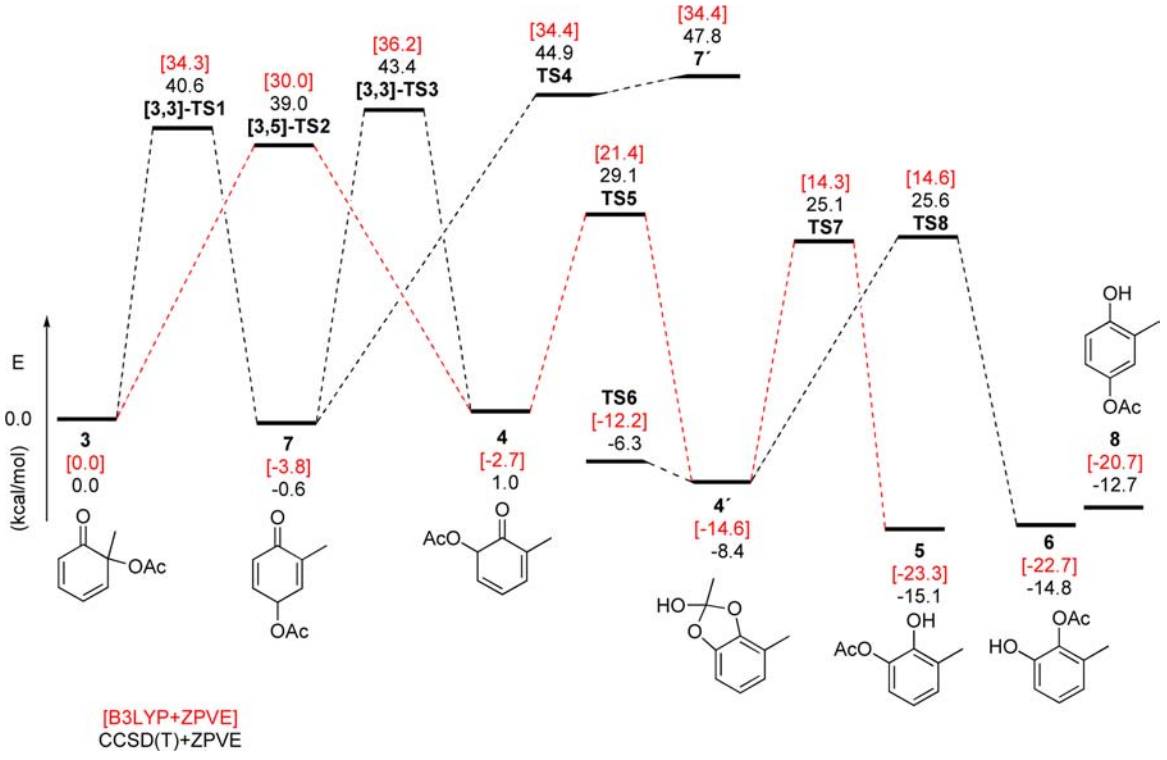

Figure 7. Calculated energy profile for the [3,3]- and [3,5]-sigmatropic rearrangements of compound **3** and subsequent reactions at the CCSD(T)/6-31G(d,p)//B3LYP/6-31G(d,p) + ZPVE level of theory; the vertical axis is approximately to scale. Relative energies at the [B3LYP/6-31G(d,p) + ZPVE] level are red and in brackets. The lowest energy pathway to compound **5** is shown in red.

bond-forming occurring in the plane of the acetate; the acetate π system is not involved.[3,4] The disconnection between the in-plane and out-of plane orbitals makes the reaction pseudopericyclic and, therefore, allowed.

These three transition states would account for the mechanisms in pathways a and b of Scheme 7. However, as discussed above, the increased selectivity for the formation of the [3,5]-sigmatropic rearrangement products **5** and **6** at higher temperatures is not consistent with these simpler mechanisms. Therefore, we searched for transition states for the required proton transfers that would lead from compound **4** to compound **5** or **6** and from compound **7** to compound **8**.

A transition structure (**TS4** in Figure 9) was located for a [1,4]-H shift from compound **7**, leading to the formation of a highly unstable zwitterionic intermediate **7′** (see Figure S5 of the Supporting Information). At the B3LYP/6-31G(d,p) level, this reaction has a comparable barrier (35.8 kcal/mol) to the other reactions from compound **7** ([3,3]-**TS1** or [3,3]-**TS3** in Figure 7). However, this proton transfer would not be productive in the gas phase, because the zwitterion **7′** is almost equally high in energy. In fact, when the ZPVE

dx.doi.org/10.1021/ja4077364 | J. Am. Chem. Soc. 2013, 135, 14438−14447

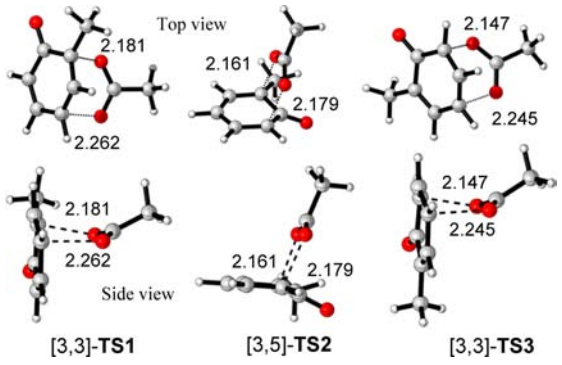

Figure 8. Top and side views of the calculated transition states for the [3,3]- and [3,5]-sigmatropic rearrangements of compound **3** at B3LYP/6-31G(d,p) optimized geometries. Distances for bond formation and bond breaking are in angstroms.

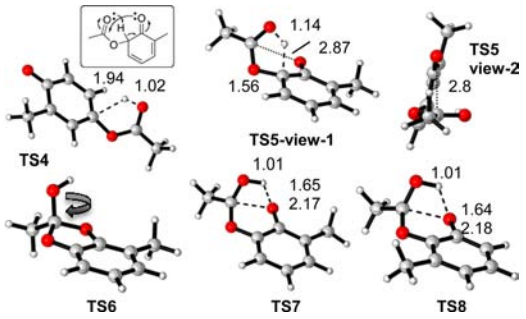

Figure 9. Calculated transition states (**TS4**–**TS8**) for the [1,4]-H shifts of the [3,3]- and [3,5]-sigmatropic rearrangement products at B3LYP/6-31G(d,p) optimized geometries, as described in Figure 7. Distances for bond formation and bond breaking are in angstroms. The inset shows an electron-pushing mechanism leading to transition state **TS5**.

correction is made, compound **7′** is higher in energy than the transition state (**TS4**); this is clearly not a physically meaningful result. The single-point energy of compound **7′** is similarly higher in energy than transition state **TS4**.

However, when a similar [1,4]-H shift was calculated for compound **4**, it resulted in a very low energy intermediate **4′** (Figure 7 and Scheme 10; 8.39 kcal/mol below compound **3**). This is formed via

Scheme 10

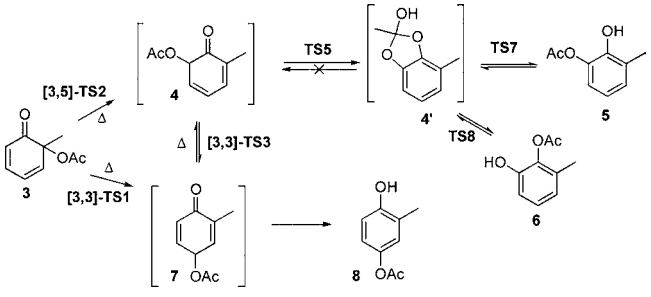

transition state **TS5** (29.12 kcal/mol), which is substantially lower in energy than [3,3]- or [3,5]-sigmatropic rearrangement transition states. This reaction provides the irreversible reaction of compound **4** required for Scheme 7c, driven by the development of aromaticity in compound **4′**. Transition state **TS5** is very asynchronous; the proton has largely transferred from C to O (C–H at 1.558 Å, versus H–O at 1.142 Å), while the forming C–O bond remains quite long (2.866 Å). At first glance, this could be considered to be a 10-electron pericyclic process (see inset in Figure 9). However, the geometry of this transition state (**TS5**) does not allow for cyclic orbital overlap; the proton is transferred in the plane of the ester carbonyl of compound **4** (horizontal in **TS5** view 2), while the new C–O bond is forming perpendicular to this plane. Therefore, the orbitals cannot overlap in a cyclic array, and therefore, the reaction is also pseudopericyclic, consistent with the low barrier observed.

The relatively low barrier calculated for the gas-phase formation of compound **4′** suggested that similar transition states might be available for the ring opening of compound **4′** to either compound **5** or **6**. Indeed, these were located (Figure 9); transition state **TS7** leads to the *o*-acetoxyphenol **5**, and transition state **TS8** leads to the isomeric phenol **6**, with barriers from compound **4′** of 33.5 and 33.9 kcal/mol, respectively. The transition state geometries are asynchronous (similar to transition state **TS5**), with the proton transfer lagging the C–O fragmentation. The geometries also suggest a pseudopericyclic mechanism, with the proton transferred out of plane of the developing phenols and the C–O bond breaking occurring in the plane of the phenols. Transition state **TS6** corresponds to rotation about the C–OH bond, allowing access to appropriate conformations, leading to both transition states **TS7** and **TS8**.

The calculated tetrahedral intermediate **4′** is the expected intermediate in acid-catalyzed transesterification (acyl migration) equilibrating compounds **5** and **6**. The synthetic utility of pH-dependent O–N acyl migrations, presumably via tetrahedral intermediates, both in peptides and for the activation of prodrugs, has been recently reviewed.[11] The possibility of a non-ionic mechanism for acyl migrations does not seem to have been suggested previously. This novel gas-phase, non-ionic mechanism may prove to be a general one for transesterification. There are reports suggesting that photochemical addition of aldehydes to *o*-quinone leads to the formation of a product described as either the *ortho*-acid ester or the phenol (Scheme 11), but the literature does not fully characterize

Scheme 11

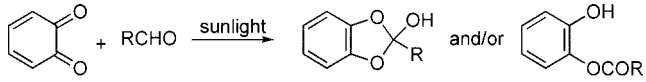

these products.[12] Our calculations strongly suggest that the *o*-acylphenol isomers would be observed products, because they are substantially more stable than the *ortho*-acid esters.

[3,3]- and [3,5]-Sigmatropic Rearrangements of Compound 9. The geometries of the ground state, products, and transition states were also calculated for the [3,5]- and the two [3,3]-sigmatropic rearrangements of compound **9**. The relative energies are summarized in Figure 10. The barrier calculated for the pseudopericyclic [3,5]-sigmatropic rearrangement of compound **9** to compound **11** ([3,5]-**TS11**) compared to the [3,3]-sigmatropic rearrangement of compound **9** to compound **14** ([3,3]-**TS9**) is slightly lower (1.9 kcal/mol) at the B3LYP/6-31G(d,p) level but slightly higher (0.3 kcal/mol) based on the CCSD(T) single-point energy calculations. The comparable barriers are in qualitative agreement with the lower yield of compound **11** in the FVP experiment. The barrier for the rearrangement of compound **14** to compound **11** is higher still (by 2.6 kcal/mol; [3,3]-**TS10** versus [3,5]-**TS11**). This suggests that compound **11** is formed primarily by the direct, pseudopericyclic [3,5]-sigmatropic rearrangement of compound **9**, despite the steric crowding of compound **11** compared to compound **14**.

[3,3]- and [3,5]-Sigmatropic Rearrangements of Compound 10. Similar calculations were performed for the [3,3]- and [3,5]-sigmatropic rearrangements of compound **10** (Figure 11). A slight preference (1.2:1 at 0.0% conversion in Figure 5) is observed experimentally for the [3,5] products (compounds **17** and **18**) over the [3,3] products (compounds **19** and **20**). The calculated barrier for the [3,3]-sigmatropic rearrangement via [3,3,]-**TS12** is slightly higher (1.8 kcal/mol) at the B3LYP level compared to the [3,5]-sigmatropic rearrangement via [3,5]-**TS14**. On the other hand, the CCSD(T) single-point energies favor the [3,3]-sigmatropic rearrangement by 1.4

dx.doi.org/10.1021/ja4077364 | J. Am. Chem. Soc. 2013, 135, 14438–14447

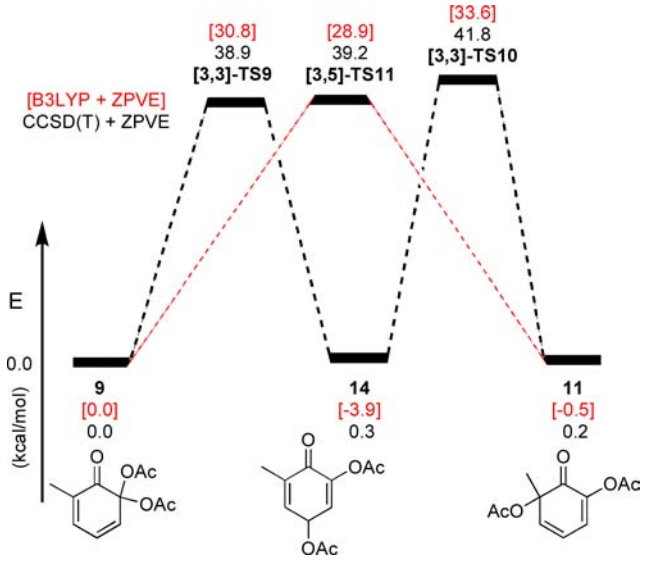

Figure 10. Calculated energy profiles for the [3,3]- and [3,5]-sigmatropic rearrangements of compound **9** at the B3LYP/6-31G(d,p) + ZPVE and CCSD(T)/6-31G(d,p)//B3LYP/6-31G(d,p) + ZPVE levels of theory.

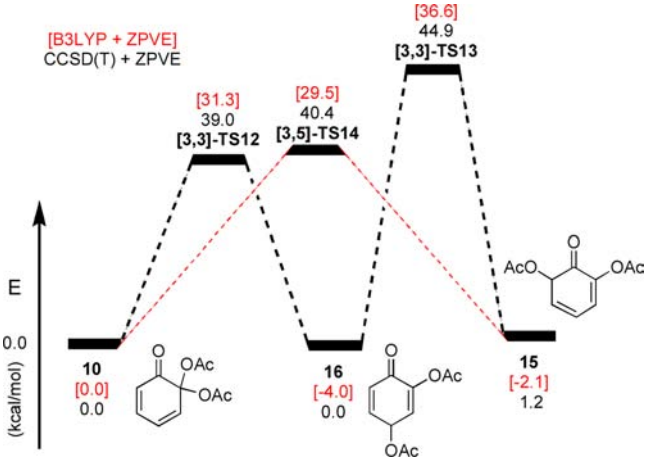

Figure 11. Calculated energy profiles for the [3,3]- and [3,5]-sigmatropic rearrangements of compound **10** at the B3LYP/6-31G(d,p) + ZPVE and CCSD(T)/6-31G(d,p)//B3LYP/6-31G(d,p) + ZPVE levels of theory.

kcal/mol; clearly the two transition states are close in energy, which is consistent with the modest experimental selectivity.

Crystal Structure Data. The three compounds **3**, **9** and **10** were crystallized to obtain high-purity samples for thermal studies. X-ray diffraction crystal structures were obtained and are shown in Figures 12, 13, and 14, respectively, along with the B3LYP/6-31G(d,p) optimized geometries of the low-energy conformations of these compounds. We were gratified to see that the calculated conformations were qualitatively similar to those of the crystals; this offers some additional validation of the calculations.

It is noteworthy that the most stable conformation places the electron-rich carbonyl oxygens over the electron-deficient ring, because this is the conformation required for the rearrangements. In the crystal structure of compound **3** (Figure 12a), both enantiomers place the carbonyl oxygen closer to the carbon involved in the [3,5]-sigmatropic rearrangement compared to that involved in the [3,3]-sigmatropic rearrangement [3.388(2) versus 3.492(2) Å or 3.511(2) versus 3.543(3) Å]. The calculations reproduce this trend as well, with the oxygen closer to the [3,5] carbon by 0.079 Å (Figure 12b).

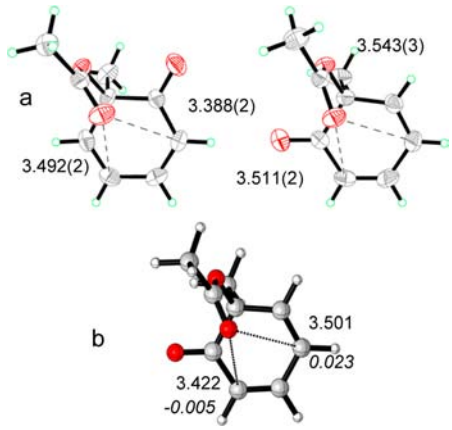

Figure 12. (a) Crystal structure of the two enantiomers of compound **3**. The thermal ellipsoids are drawn at the 50% probability level. (b) Most stable conformation of compound **3** as calculated at the B3LYP/6-31G(d,p) level of theory. Distances are in angstroms. Mulliken charges with hydrogens summed to heavy atoms are shown in italics.

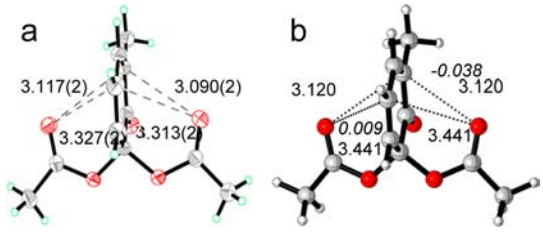

Figure 13. (a) Crystal structure of compound **9**. The thermal ellipsoids are drawn at the 50% probability level. (b) Most stable conformation of compound **9** as calculated at the B3LYP/6-31G(d,p) level of theory. Mulliken charges with hydrogens summed to heavy atoms are shown in italics.

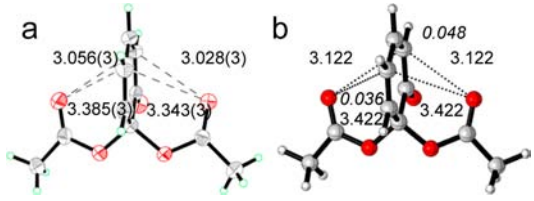

Figure 14. (a) Crystal structure of compound **10**. The thermal ellipsoids are drawn at the 50% probability level. (b) Most stable conformation of compound **10** as calculated at the B3LYP/6-31G(d,p) level of theory. Mulliken charges with hydrogens summed to heavy atoms are shown in italics.

This appears not to be a coincidence in the case of compound **3**; compounds **9** and **10** show similar distortions. The crystal structure of compound **9** is shown in Figure 13a. The two carbonyl groups are not symmetrically positioned, but in this crystal structure as well, the distances are significantly shorter to the [3,5] carbon than those to the [3,3] carbon [3.090(2) versus 3.313(2) Å and 3.117(2) versus 3.327(2) Å]. The calculated structure is symmetrical but also reflects the closer approach of the carbonyl oxygen to the [3,5] carbon (3.120 versus 3.441 Å in Figure 13b).

The crystal structure of compound **10** (Figure 14a) shows similar trends. Again, the distances to the [3,5] carbon are significantly shorter than those to the [3,3] carbon [3.056(3) versus 3.385(3) Å and 3.028(3) versus 3.343(3) Å]. The calculated structure also reflects the closer approach of the carbonyl oxygen to the [3,5] carbon (3.122 versus 3.442 Å in Figure 14b).

The geometry does not appear to be a consequence of electrostatics; in compounds **3**, **9**, and **10**, the migration termini for

dx.doi.org/10.1021/ja4077364 | J. Am. Chem. Soc. 2013, 135, 14438−14447

the [3,5]-sigmatropic rearrangements are calculated to be less positively charged and, hence, would be expected to attract the carbonyl lone pair less strongly than for the [3,3]-sigmatropic rearrangements. In addition, in all three structures (compounds **3**, **9**, and **10**), it is the lone pair and not the π system of the ester that is pointed toward the carbon. It would be this lone pair that is calculated to be involved in bond formation in the pseudopericyclic [3,5]-sigmatropic rearrangement. While closer approach of the carbonyl oxygens to the carbon to which they will bond in the [3,5]-sigmatropic rearrangements does not in itself require that the eight-centered pseudopericyclic pathway be followed, both the distances and the lone-pair orientations of the carbonyls in the crystal structures prefigure the calculated pseudopericyclic [3,5]-sigmatropic rearrangement transition states. These are in accordance with the structure−reactivity correlation by Bürgi and Dunitz, which suggests that ground states tend to distort along allowed reaction coordinates.[4e,13,14]

CONCLUSION

The combined experimental and computational studies reported here provide strong evidence that the [3,5]-sigmatropic rearrangements of esters are allowed via a pseudopericyclic pathway and are kinetically favored (at 0.0% conversion) over the more familiar [3,3]-sigmatropic rearrangements. The thermal rearrangements of two 6-acetoxy-2,4-cyclohexadienones **3** and **10** were investigated by FVP at temperatures ranging from 300 to 500 °C. For each reaction, the ratio of [3,5]/[3,3] products (isolated after tautomerization to the corresponding phenols) gives a straight line when plotted versus percent conversion, between 300 and approximately 400 °C. When extrapolated to 0.0% conversion, the initial ratio for compound **3** is 3.17:1, and for compound **10**, it is 1.2:1, favoring the [3,5]-sigmatropic rearrangement products in both cases. A pericyclic [3s,5s]-sigmatropic rearrangement would be orbital-symmetry-forbidden, but the ester rearrangement is allowed via a pseudopericyclic transition state, in which bond breaking and forming occurs in the plane of the ester. These transition states are prefigured by the ground-state geometries from X-ray crystal structures of compounds **3**, **9**, and **10**. The immediate product from [3,5]-sigmatropic rearrangement of compound **9** is compound **11**, and this compound can be isolated without tautomerization. DFT calculations also predict pseudopericyclic transition states and reproduce the qualitative preference for [3,5]-sigmatropic rearrangements.

As the FVP temperature is raised and, particularly, at temperatures above 400 °C, the selectivity for the [3,5]-sigmatropic rearrangement products increases. This unusual situation can be explained by invoking a non-ionic (gas-phase) pathway for the formation of a tetrahedral intermediate (*ortho*-acid ester **4′**) that is formed irreversibly from compound **4** via another pseudopericyclic transition state **TS-5**. Thus, at higher temperatures, compounds **3**, **4**, and **7** are approaching equilibrium, but the irreversible reaction to form **4′** shifts the equilibrium. This intermediate (**4′**) can then open via a similar transition state to give either isomeric *o*-acetoxyphenol (**5** or **6**). This may be a general mechanism for acyl migrations.

ASSOCIATED CONTENT

Supporting Information

Experimental information, including synthetic procedures, FVP and GC conditions, ^{1}H and ^{13}C NMR spectra of all new compounds, details of X-ray crystal structures, and computational information, including energies, pictures, and Cartesian coordinates of all conformations of all calculated structures. This material is available free of charge via the Internet at http://pubs.acs.org.

AUTHOR INFORMATION

Corresponding Author

david.birney@ttu.edu

Present Address

‡David B. Cordes: EaStCHEM, School of Chemistry, University of St. Andrews, North Haugh, St. Andrews, Fife KY16 9ST, United Kingdom.

Author Contributions

†Shikha Sharma and Trideep Rajale contributed equally to this work.

Notes

The authors declare no competing financial interest.

ACKNOWLEDGMENTS

We gratefully acknowledge generous support from the Robert A. Welch Foundation (Grant D-1239). We also are grateful for the use of a 400 MHz MNH spectrometer made available through the NSF CRIF MU Grant CHE-1048553 and access to the Robinson cluster, which is funded by CRIF MU Instrumentation Grant CHE-0840493 from the National Science Foundation. Both instruments are in the Department of Chemistry and Biochemistry, Texas Tech University. We thank Professor Stephane Quideau for introducing us to Wessely's chemistry, David Purkiss for assistance with the NMR spectra, Dr. George Tamas for assistance with electronic structure theory calculations, and Daniel A. Stroud for synthetic assistance.

REFERENCES

(1) (a) Woodward, R. B.; Hoffmann, R. *The Conservation of Orbital Symmetry*; Verlag Chemie GmbH: Weinheim, Germany, 1970. (b) Woodward, R. B.; Hoffmann, R. *Angew. Chem.* **1969**, *81*, 797−869; *Angew. Chem., Int. Ed. Engl.* **1969**, *8*, 781−853.

(2) Leach, A. G.; Catak, S.; Houk, K. N. *Chem.—Eur. J.* **2002**, *8*, 1290−1299.

(3) Ross, J. A.; Seiders, R. P.; Lemal, D. M. *J. Am. Chem. Soc.* **1976**, *98*, 4325−4327.

(4) (a) Birney, D. M.; Wagenseller, P. E. *J. Am. Chem. Soc.* **1994**, *116*, 6262−6270. (b) Birney, D. M.; Ham, S.; Unruh, G. R. *J. Am. Chem. Soc.* **1997**, *119*, 4509−4517. (c) Birney, D. M.; Xu, X.; Ham, S. *Angew. Chem., Int. Ed.* **1999**, *38*, 189−193. (d) Quideau, S.; Looney, M. A.; Pouységu, L.; Ham, S.; Birney, D. *Tetrahedron Lett.* **1999**, *40*, 615−618. (e) Shumway, W. W.; Dalley, N. K.; Birney, D. M. *J. Org. Chem.* **2001**, *66*, 5832−5839. (f) Wei, H.-X.; Zhou, C.; Ham, S.; White, J. M.; Birney, D. M. *Org. Lett.* **2004**, *6*, 4289−4292. (g) Gudipati, I. R.; Sadasivam, D. V.; Birney, D. M. *Green Chem.* **2008**, *10*, 283−285. (h) Sadasivam, D. V.; Birney, D. M. *Org. Lett.* **2008**, *10*, 245−248. (i) Ji, H.; Li, L.; Xu, X.; Ham, S.; Hammad, L. A.; Birney, D. M. *J. Am. Chem. Soc.* **2009**, *131*, 528−537. (j) Birney, D. M. *Curr. Org. Chem.* **2010**, *14* (15), 1658−1668.

(5) (a) Quideau, S. *ChemBioChem* **2004**, *4*, 427−430. (b) Pouységu, L.; Deffieux, D.; Quideau, S. *Tetrahedron* **2010**, *66*, 2235−2261. (c) Pouységu, L.; Sylla, T.; Garnier, T.; Rojas, L. B.; Charris, J.; Deffieux, D.; Quideau, S. *Tetrahedron* **2010**, *66*, 5908−5917. (d) Fujiwara, K.; Sato, T.; Sano, Y.; Norikura, T.; Katoono, R.; Suzuki, T.; Matsue, H. *J. Org. Chem.* **2012**, *77*, 5161−5166.

(6) (a) Metlesics, W.; Schinzel, E.; Vilcsek, H.; Wessely, F. *Monatsh. Chem.* **1957**, *88*, 1069−1076. (b) Siegel, A.; Wessely, F.; Stockhammer, P.; Antony, F.; Klezl, P. *Tetrahedron* **1958**, *4*, 49−67. (c) Budzikiewicz, H.; Metlesics, W.; Wessely, F. *Monatsh. Chem.* **1960**, *91*, 117−128. (d) Zbiral, E.; Wessely, F.; Lahrmann, E. *Monatsh. Chem.* **1960**, *91*, 331−347. (e) Zbiral, E.; Wessely, F.; Thermische, J. J.

Monatsh. Chem. **1961**, *92*, 654−666. (f) Wessely, F.; Takacs, F. *Monatsh. Chem.* **1964**, *95*, 222−230.
(7) (a) Yranzo, G. I.; Elguero, J.; Flammang, R.; Wentrup, C. *Eur. J. Org. Chem.* **2001**, 2209−2220. (b) McNab, H. *Aldrichimica Acta* **2004**, *37*, 19. (c) McNab, H. *Contemp. Org. Synth.* **1996**, *3*, 373−396.
(8) Li, D.; Park, J.; Oh, J.-R. *Anal. Chem.* **2001**, *73*, 3089−3095.
(9) (a) Frisch, M. J.; et al. *Gaussian 03, Revision C.02*; Gaussian, Inc.: Wallingford, CT, 2004 (see the Supporting Information for the full citation). (b) B3LYP method: Becke, A. D. *J. Chem. Phys.* **1993**, *98*, 5648−5652. (c) 6-31G(d,p) basis set: Hariharan, P. C.; Pople, J. A. *Theor. Chim. Acta* **1973**, *28*, 213. There are limitations to the B3LYP method; see for example: (d) Schreiner, P. R.; Fokin, A. A.; Pascal, R. A., Jr.; de Meijere, A. *Org. Lett.* **2006**, *8*, 3635−3638. (e) Wodrich, M. D.; Corminboeuf, C.; von Ragué Schleyer, P. *Org. Lett.* **2006**, *8*, 3631−3634. However, there are also examples, particularly for orbital-symmetry-allowed reactions, where B3LYP is well-suited: (f) Birney, D. M. *J. Am. Chem. Soc.* **2000**, *122*, 10917−10925. (g) Guner, V.; Khuong, K. S.; Leach, A. G.; Lee, P. S.; Bartberger, M. D.; Houk, K. N. *J. Phys. Chem. A* **2003**, *107*, 11445−11459.
(10) (a) NWChem: Valiev, M.; Bylaska, E.; Govind, N.; Kowalski, K.; Straatsma, T.; Van Dam, H.; Wang, D.; Nieplocha, J.; Apra, E.; Windus, T.; de Jong, W. A. *Comput. Phys. Commun.* **2010**, *181*, 1477−1489. CCSD(T): (b) Bartlett, R. J.; Purviss, G. D., III. *Int. J. Quantum Chem.* **1978**, *14*, 561−581. (c) Pople, J. A.; Krishnan, R.; Schlegel, H. B.; Binkley, J. S. *Int. J. Quantum Chem.* **1978**, *14*, 545−560. (d) Pople, J. A.; Head-Gordon, M.; Raghavachari, K. *J. Chem. Phys.* **1987**, *87*, 5968−5975.
(11) (a) Skwarczynski, M.; Kiso, Y. *Curr. Med. Chem.* **2007**, *14*, 2813−2823. (b) Lee, T.-K.; Anh, J.-M. *ACS Comb. Sci.* **2011**, *13*, 107−111. (c) Hydroxide-catalyzed O−O acyl migrations are known in sugar chemistry: Nicholls, A. W.; Akira, K.; Lindon, J. C.; Farrant, R. D.; Wilson, I. D.; Hardin, J.; Killick, D. A.; Nicholson, J. K. *Chem. Res. Toxicol.* **1996**, *9*, 1414−1424.
(12) (a) Schönberg, A.; Awad, W. I.; Mousa, G. A. *J. Am. Chem. Soc.* **1955**, *77*, 3850−3852. (b) Mustafa, A.; Harhash, A. H. E.; Mansour, A. K. E.; Omran, S. M. A. E. *J. Am. Chem. Soc.* **1956**, *78*, 4306−4309. (c) Mustafa, A.; Mansour, A. K.; Shalaby, A. F. A. M. *J. Am. Chem. Soc.* **1959**, *81*, 3409−3413. (d) Mustafa, A.; Mansour, A. K.; Zaher, H. A. A. *J. Org. Chem.* **1960**, *25*, 949−950.
(13) Bürgi, H. B.; Dunitz, J. D. *Acc. Chem. Res.* **1983**, *16*, 153−161.
(14) Birney, D. M.; Lim, T. K.; Koh, J. H. P.; Pool, B. R.; White, J. M. *J. Am. Chem. Soc.* **2002**, *124*, 5091−5099.